

A Dual-Stage Reconstruction Algorithm for Magnetic Resonance Elastography

E. E. Van Houten¹, and R. Sinkus²

¹Department of Mechanical Engineering, University of Canterbury, Christchurch, Canterbury, New Zealand, ²Laboratoire Ondes et Acoustique, l'Ecole Supérieure de Physique et de Chimie Industrielles, Paris, France

METHODS

Spin echo encoded, steady-state harmonic motion data was collected from a cylindrical, gelatine phantom containing multiple inclusions in order to test a dual-stage Magnetic Resonance Elastography (MRE) reconstruction approach. This reconstruction method uses a viscoelastic shear modulus distribution calculated from derivatives of filtered displacement values as an initial guess for an iterative calculation of the Rayleigh damping parameters which provide a best fit to the undifferentiated, unfiltered data. Both stages of the reconstruction algorithm are based on the assumption of a linear elastic material governed by Navier's equation for time harmonic displacements:

$$\nabla \cdot (\mu \nabla \mathbf{u}) + \nabla ((\lambda + \mu) \nabla \cdot \mathbf{u}) = -\rho \omega^2 \mathbf{u} \quad (1)$$

STAGE ONE of this reconstruction method looks to calculate a complex valued shear modulus, $\mu = \mu_R + i\mu_I$, by using the measured displacements, \mathbf{u} , as known values in eq. (1). This calculation requires a number of initial steps and assumptions. To begin with, the first term on the left-hand-side of eq. (1) can be simplified by the so-called *local homogeneity* assumption, where:

$$\nabla \mu \cdot \nabla \mathbf{u} \approx \mathbf{0}, \text{ so that } \nabla \cdot (\mu \nabla \mathbf{u}) \approx \mu \nabla^2 \mathbf{u} \quad (2)$$

The second issue in using eq. (1) to generate solutions for μ is the additional unknown Lamé's constant, λ , which describes the compressional wave behaviour within the material. Given the high speed of these waves in nearly incompressible media, these dynamics are not well captured by the MR motion encoding, and thus these terms are removed from eq. (1) by applying the curl operator to both sides of the equation. The combination of this step and the approximation shown in eq. (2) leads to:

$$\mu \nabla^2 \mathbf{q} = -\rho \omega^2 \mathbf{q}, \text{ where } \mathbf{q} = \nabla \times \mathbf{u} \quad (3)$$

This in turn leads to the so-called *direct* solution for μ in terms of \mathbf{q} :

$$\mu = \frac{-\rho \omega^2 \mathbf{q}}{\nabla^2 \mathbf{q}} \quad (4)$$

STAGE TWO of this reconstruction process seeks to correct for two steps required to generate the solution shown in eq. (4), namely the use of the local homogeneity assumption seen in eq. (2) and the filtering of the measured data required to reduce noise amplification effects from the 3rd order differentiation implicit in the denominator term of eq. (4). This correction is achieved by using the solution for μ in eq. (4) as an initial guess for a model-based, non-linear, iterative optimisation process to find a set of complex valued parameters, μ and ρ , such that:

$$(\mu, \rho) = \arg \min \|\mathbf{u}^c(\mu, \rho) - \mathbf{u}\|^2 \quad (5)$$

where \mathbf{u}^c is a set of displacements calculated for the current estimate of μ and ρ based on finite element discretization of eq. (1), which allows for local heterogeneity in the shear modulus parameter, μ . Additionally, by using untreated measurement data for the displacements, \mathbf{u} , in eq. (5), this second stage can avoid the necessity of filtering the measured motions.

RESULTS

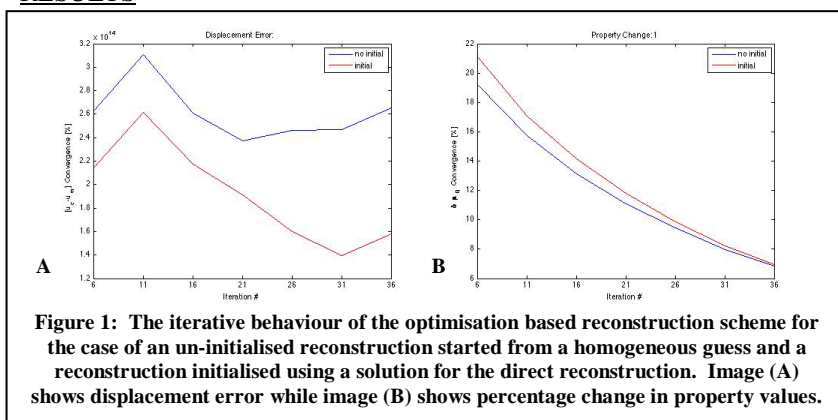


Figure 1: The iterative behaviour of the optimisation based reconstruction scheme for the case of an un-initialised reconstruction started from a homogeneous guess and a reconstruction initialised using a solution for the direct reconstruction. Image (A) shows displacement error while image (B) shows percentage change in property values.

Results from elastic property reconstruction performed on the cylindrical, multi-inclusion gelatine phantom indicate that the use of an initial solution from the direct reconstruction shown in eq. (4) improves both the overall displacement error for the iterative optimisation method (fig. 1A), and the rate of convergence for the iterative solution (fig. 1B). Fig. 2 shows the property distributions across a central slice through the phantom. Fig. 2A shows the initial direct solution used in the optimisation based reconstruction algorithm, while fig. 2B shows the solution from at iteration 20 of the un-initialised optimisation process and fig. 2C shows the solution at iteration 20 of the initialised optimisation process.

CONCLUSIONS

The two stage reconstruction process shows clear improvements over the use of either stage as an independent MRE reconstruction method. Fig. 2A clearly shows the low stiffness artefact that typically surrounds hard inclusions reconstructed with the local homogeneity assumption, which is not present in the final solution of the two stage reconstruction seen in fig. 2C. Likewise fig. 2B, when compared with fig. 2C, shows how the use of an initial solution improves the speed of convergence in the iterative solution.

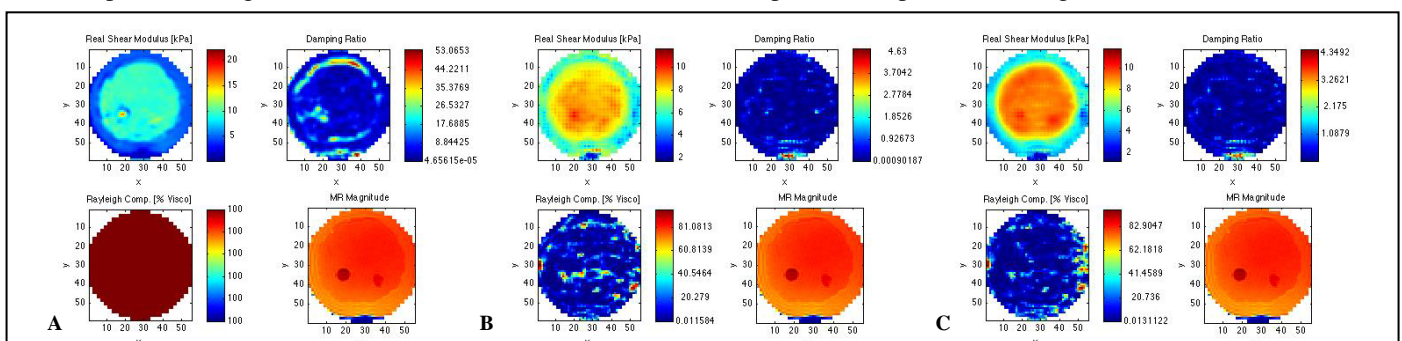


Figure 2: Results of the iterative reconstruction process: the initial solution from the direct reconstruction (A); the solution from iteration 20 of the un-initialised optimisation based reconstruction (B); the solution from the initialised optimisation based reconstruction (C).